Persistent breather excitations in an ac-driven sine-Gordon system with loss

P. S. Lomdahl and M. R. Samuelsen*
Theoretical Division and Center for Nonlinear Studies, Los Alamos National Laboratory, University of California, P.O. Box 1663, Los Alamos, New Mexico 87545
(Received 5 December 1985)

In a sine-Gordon system with loss and applied ac driver, a breather can be maintained as a persistent entrained oscillation if the driver is strong enough. The threshold field is determined by a perturbation method and compared to numerical experiments. Excellent agreement is found.

I. INTRODUCTION

Soliton solutions to the sine-Gordon equation model many physical phenomena. The 2π-kink soliton models the motion of dislocations in crystals, domain walls in ferromagnets, flux quanta, and fluxons in Josephson transmission lines.[1] The other type of soliton solution, the breather (an oscillating bound kink-antikink pair), will in real physical systems decay away because of dissipation. If an ac force is added to the sine-Gordon system it can compensate for the losses and maintain a stationary breather[2-4]—or even excite a breather—with a frequency equal to the applied frequency.

It is the purpose of this paper to present a perturbation calculation of the threshold for the applied force to keep the breather alive. Several perturbation treatments of sine-Gordon breathers have been presented,[5-7] used in different contexts,[8-10] and compared to numerical experiments.[8-14] The difficulty in using perturbation methods on breathers subjected to general perturbations, is that even small perturbations of the sine-Gordon equation yield drastic variations of the breathers parameters within one breather period. This problem does not seem to exist in the case of a steady-state oscillating breather, which is considered here.

The method used first divides the solution into two parts, a breather part $\phi^{\rm br}(x,t)$, and a homogeneous part $\phi^{\rm vac}(t)$, which is the solution at $x=\pm\infty$, or the solution if no breather is present; second, we use the energy considerations. The only approximation made consists of choosing the pure sine-Gordon breather for $\phi^{\rm br}(x,t)$,

$$\phi_0^{\rm br}(x,t)=4\arctan\left[\frac{(1-\omega_B^2)^{1/2}}{\omega_B}\frac{\cos(\omega_B t+\theta_{\rm br})}{\cosh[(1-\omega_B^2)^{1/2}x]}\right] . \tag{1}$$

The same kind of method has given excellent results for the 2π-kink motion with[15] and without[16] applied forces.

The outline of the paper is as follows. In Sec. II we develop the perturbation result and compare it with numerical simulations in Sec. III. Finally in Sec. IV we summarize and conclude.

II. ANALYSIS

The equation considered here is a perturbed sine-Gordon equation

$$\phi_{xx}-\phi_{tt}=\sin\phi+\alpha\phi_t-\eta\sin(\omega t) , \tag{2}$$

where α is the loss parameter, η the amplitude of the external ac force, and $\omega/2\pi$ its frequency. We define the energy as

$$H=\int[\tfrac{1}{2}\phi_x^2+\tfrac{1}{2}\phi_t^2+(1-\cos\phi)]dx . \tag{3}$$

For the pure sine-Gordon breather [Eq. (1)] this energy is

$$H_0=16(1-\omega_B^2)^{1/2} . \tag{4}$$

In the general case time differentiation of Eq. (3) and the use of Eq. (2) yields

$$\frac{dH}{dt}=-\alpha\int\phi_t^2\,dx+\eta\sin(\omega t)\int\phi_t\,dx . \tag{5}$$

The integration is over the length L of the system and the following boundary condition has to be fulfilled

$$\phi_x\left[-\frac{L}{2},t\right]\phi_t\left[-\frac{L}{2},t\right]=\phi_x\left[\frac{L}{2},t\right]\phi_t\left[\frac{L}{2},t\right] . \tag{6}$$

The condition is fulfilled if $\phi_x(\pm L/2,t)=0$, or with periodic boundary conditions and breather symmetry, or if $L=\infty$.

The change in energy in a given time interval may be found by integrating Eq. (5) over this time interval

$$\Delta H=-\alpha\int\int\phi_t^2\,dx\,dt+\eta\int\sin(\omega t)\int\phi_t\,dx\,dt . \tag{7}$$

In a stationary case this change in energy is zero for one period.

The method we use is first to divide the solution to Eq. (2) into two parts

$$\phi(x,t)=\phi^{\rm br}(x,t)+\phi^{\rm vac}(t) , \tag{8}$$

where $\phi^{\rm vac}(t)$ is the solution for $x=\pm\infty$. $\phi^{\rm vac}(t)$ does not depend on the presence of the breather. $\phi^{\rm br}(x,t)$ is the localized breather $[\phi^{\rm br}(\pm\infty,t)=0]$. Next we insert Eq. (8) into Eq. (7) and get

$$\Delta H\equiv I_1+I_2+I_3+I_4+I_5 , \tag{9}$$

where

$$I_1=-\alpha\int\int(\phi_t^{\rm br})^2\,dx\,dt ,$$

$$I_2=-\alpha\int\int(\phi_t^{\rm vac})^2\,dx\,dt\ ,$$

$$I_3=-2\alpha\int dt\,\phi_t^{\rm vac}\int dx\,\phi_t^{\rm br}\ ,$$

$$I_4=\eta\int dt\sin(\omega t)\int dx\,\phi_t^{\rm br}\ ,$$

$$I_5=\eta\int\int\sin(\omega t)\phi_t^{\rm vac}dx\,dt\ .$$

Each of the five terms in Eq. (9) can be given a very simple physical interpretation as shown in Fig. 1. The losses from the breather part and the homogeneous part are given by I_1 and I_2, respectively. The drivers energy input to the breather and the homogeneous part is given by I_4 and I_5, respectively. I_3 represents the energy flow from the homogeneous part to the breather part. Far away from the breather only I_2 and I_5 are different from zero, therefore these two divergent terms will cancel.

Until now no approximation has been made. Only in the small signal limit can we give a closed solution for the homogeneous part. Then it is just a forced damped harmonic oscillator:

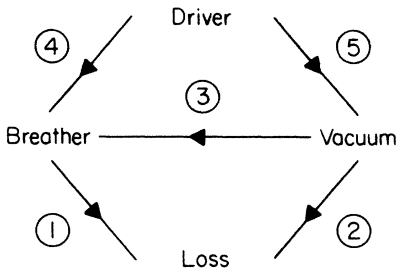

FIG. 1. A schematical representation of the energy flow given by the different terms in Eq. (9).

$$\phi^{\rm vac}(t)=\frac{\eta}{[(1-\omega^2)^2+\alpha^2\omega^2]^{1/2}}\sin(\omega t-\theta)\ ,$$
$$\tan\theta=\frac{\alpha\omega}{1-\omega^2}\ . \tag{10}$$

This approximation is easy to estimate ($1-\omega^2>\alpha\omega$).

The energy input to the breather part, I_3 and I_4 in Eq. (9), now adds up to

$$I_3+I_4=\eta\int dt\left[\sin(\omega t)-\frac{2\alpha\omega}{[(1-\omega^2)^2+\alpha^2\omega^2]^{1/2}}\cos(\omega t-\theta)\right]\int dx\,\phi_t^{\rm br}=\eta\int dt\sin(\omega t-2\theta)\int dx\,\phi_t^{\rm br}\ . \tag{11}$$

We notice that Eq. (11)— except for the phase angle 2θ— is the same as term 4 in Eq. (9). This means that for the perturbation result we could as well neglect I_3 in Eq. (9) (the interaction between the breather part and the homogeneous part), but to get the best initial conditions for the numerical simulation it was crucial to keep the phase angle 2θ in Eq. (11).

Close to the threshold we should have the maximum energy input from Eq. (11), i.e.,

$$\phi_t^{\rm br}\sim\sin(\omega t-2\theta) \tag{12}$$

or

$$\phi^{\rm br}\sim\cos(\omega t+\pi-2\theta)\ . \tag{13}$$

Therefore close to the threshold the phase of the breather should be $\pi-2\theta$. The phases of the applied force [$\sin(\omega t)$], the homogeneous part $\phi^{\rm vac}(t)$, and the breather part are shown in Fig. 2. The breather loss [I_1 in Eq. (9)] is independent of the breather phase. The threshold force $\eta_{\rm th}$ is determined when Eq. (11) (I_3+I_4) and I_1 cancel. For larger forces the terms still cancel because the breather phase adjusts accordingly.

The *main approximation* we make is to choose the sine-Gordon breather of Eq. (1) for $\phi^{\rm br}(x,t)$ with $\omega_B=\omega$. We now do the integrals for the time over one period ($2\pi/\omega$) and for the spatial variable from $-L/2$ to $L/2$. The integral [Eq. (11)] for the energy input to the breather can only be done exactly for $L=\infty$. For large L we find ($\omega\neq 0$ and 1)

$$I_3+I_4\cong\frac{16\pi\eta}{1-\omega^2}[K(1-\omega^2)-E(1-\omega^2)]-\frac{8\pi\eta}{\omega\sinh\left[(1-\omega^2)^{1/2}\frac{L}{2}\right]}\ , \tag{14}$$

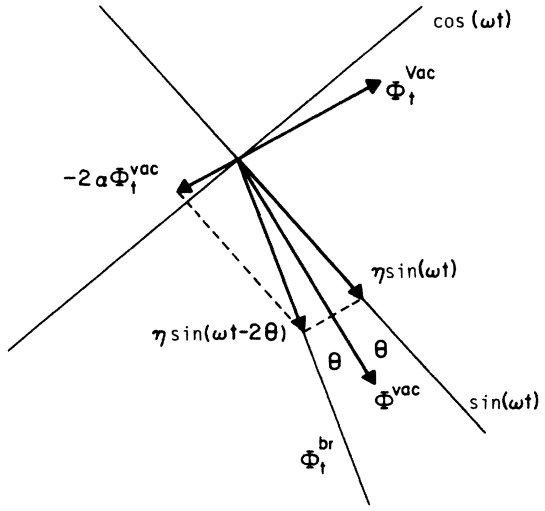

FIG. 2. A diagram showing the selective phases of the applied force [$\sin(\omega t)$], the homogeneous part $\phi^{\rm vac}(t)$, and the breather part $\phi^{\rm br}(x,t)$ of the solution close to the threshold for $\alpha=0.2$ and $\omega=0.6$.

where K and E are complete elliptic integrals of the first and the second kind, respectively.[17]

The integrals for the breather energy loss I_1 can be carried through. The result is ($\omega \neq 0$ and 1)

$$I_1 = -32\pi\alpha \sin^{-1}\left\{[(1-\omega^2)^{1/2}]\sin\left\{\tan^{-1}\left[\sinh\left[(1-\omega^2)^{1/2}\frac{L}{2}\right]\right]\right\}\right\}$$

$$\cong -32\pi\alpha \sin^{-1}[(1-\omega^2)^{1/2}] + \frac{16\pi\alpha}{\omega}\frac{(1-\omega^2)^{1/2}}{\sinh^2\left[(1-\omega^2)^{1/2}\frac{L}{2}\right]} . \tag{15}$$

Therefore we find, for a long sine-Gordon system with driving frequencies not too close to $\omega=1$ [Eq. (10)] and $\omega=0$, the following expression for the force threshold:

$$\eta_{\rm th} = \frac{2\alpha(1-\omega^2)\sin^{-1}[(1-\omega^2)^{1/2}]}{K(1-\omega^2)-E(1-\omega^2)} . \tag{16}$$

Equation (16) is shown in Fig. 3 as the solid curve.

In the next section we will compare the perturbation result Eq. (16) with numerical simulations where the combination of α, ω, and L is such that the linearization in Eq. (10) is valid and the length corrections in Eqs. (14) and (15) can be neglected.

III. NUMERICAL SIMULATIONS

Numerical simulations of the perturbed sine-Gordon equation [Eq. (2)] have been performed for a system of length $L=24$ and periodic boundary conditions. For this length the corrections in Eqs. (14) and (15) are negligible and high-frequency breathers ($\omega=0.9$) are well accommodated. As an initial condition we have chosen Eq. (8) with Eq. (10) for $\phi^{\rm vac}(t)$ and $\phi_0^{\rm br}(x,t)$ of Eq. (1) for $\phi^{\rm br}(x,t)$ with $\theta_{\rm br}$ [Eqs. (1) and (13)] determined by

$$\theta_{\rm br} = \pi - 2\theta . \tag{17}$$

If we define $\phi^0(x,t)$ as

$$\phi^0(x,t) = 4\arctan\left[\frac{(1-\omega^2)^{1/2}}{\omega}\frac{\cos(\omega t+\pi-2\theta)}{\cosh[(1-\omega^2)^{1/2}x]}\right] + \frac{\eta}{[(1-\omega^2)^2+\alpha^2\omega^2]^{1/2}}\sin(\omega t-\theta) , \tag{18}$$

$$\tan\theta = \frac{\alpha\omega}{1-\omega^2} ,$$

then our initial conditions are

$$\phi(x,0)=\phi^0(x,0) \quad \text{and} \quad \phi_t(x,0)=\phi_t^0(x,0) . \tag{19}$$

In all numerical experiments the breather and the vacuum were found to lock to the driving frequency consistent with the choice of ω in Eq. (18). The time evolution was followed for as long a time as necessary to decide whether the breather survived or decayed. For $\eta < \eta_1$ the breather decayed into a spatially homogeneous flat state. For $\eta > \eta_2$ the breather was maintained as a persistent oscillating structure quite similar to the analytical solution [Eq. (1)] of the unperturbed sine-Gordon equation. η_1 and η_2 indicate the uncertainty on the numerically determined $\eta_{\rm th}$. For $\eta \gg \eta_2$ the breather gained so much energy that it broke up into a kink-antikink pair.[9] This scenario (with three basins of attraction) has been followed for $\omega=0.2$, 0.4, 0.6, 0.8, and 0.9 with $\alpha=0.04$, 0.1, and 0.2. The results are shown in Fig. 3 as bars, with heights determined by η_1 and η_2. The numerical results agree very well with the perturbation results [Eq. (16)]. There is only one deviation and that occurs where expected: large damping ($\alpha=0.2$) and frequency ($\omega=0.9$). For medium frequencies we find that the breather survived for a relatively wide range of η values ($\geq \eta_{\rm th}$), while for $\omega=0.2$ the breather survived only in a narrow range of η values, and for $\omega=0.1$ we were not able to maintain the breather at all.

We note that the numerical result depends critically on the initial condition Eq. (19). For instance for $\alpha=0.2$ and $\omega=0.6$, we find $\eta_{\rm th}=0.33$ both from perturbation theory and from numerical simulation as is also found in Ref. 14. In Refs. 2 and 3 $\eta_{\rm th}=0.57$ is found numerically from a slightly different initial condition. For smaller frequencies the sensitivity to the initial condition becomes even stronger.

The reason for the high sensitivity to the initial condition is that the energy flow per period—along the different channels in Fig. 1—are comparable to the energy of the breather or the binding energy of the kink-antikink pair $16\text{-}H_0$ [see Eq. (4)]. For instance for $\alpha=0.2$ and $\omega=0.6$, the loss (and therefore energy input) for the breather in one period is 18.81. A little imbalance in the initial conditions could therefore cause the breather to decay or break up into a kink-antikink pair in the first period.

Another observation from the numerical experiment was that for $\omega=0.8$ and $\omega=0.9$, just a little above $\eta_{\rm th}$ two breathers instead of the initial one breather were maintained. This spatial period halving was also observed in Refs. 2 and 3.

IV. CONCLUDING REMARKS

We have used a perturbation method based on energy flow to predict the threshold value of an ac driver for maintaining persistent breather oscillations. We find very good agreement with numerical simulations. We have not been able to extend our energy-flow perturbation method to predict other interesting transitions known to exist for the damped ac-driven sine-Gordon system.[2–4,14] This scenario includes spatial period halving and quartering, intermittency, and low-dimensional chaos. It is clear that

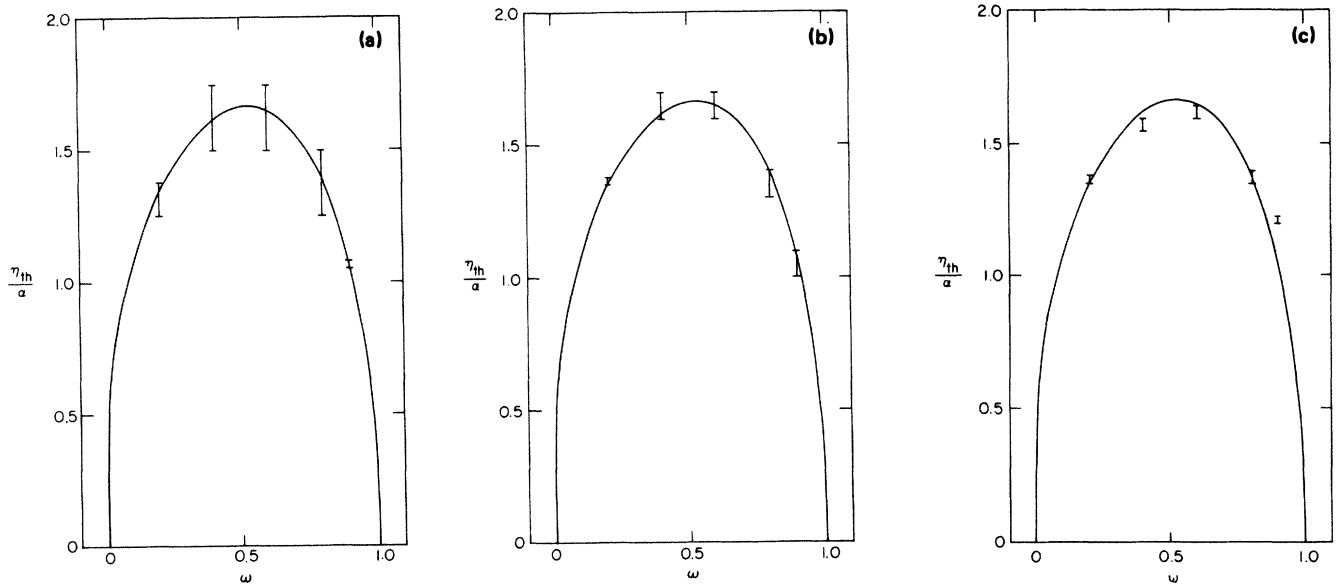

FIG. 3. The threshold force η_{th} vs the cyclic frequency ω for various values of the loss parameter α. (a) $\alpha=0.04$, (b) $\alpha=0.1$, and (c) $\alpha=0.2$. Shown is η_{th}/α. The solid curve is the perturbation result [Eq. (16)] and the bars are the results of the numerical simulations (see the text).

the dynamics often is governed by only a few collective "soliton" modes and that strong mode-locking takes place.[4,14] It should therefore be interesting to see if perturbation methods will be able to predict transitions in these fully developed nonlinear regimes.

ACKNOWLEDGMENTS

One of us (M.R.S.) thanks the Center for Nonlinear Studies for its hospitality. The work was done under the auspices of the U.S. Department of Energy.

*Permanent address: Physical Laboratory I, The Technical University of Denmark, DK-2800 Lyngby, Denmark.

[1]A. Barone, F. Esposito, C. J. Magee, and A. C. Scott, Riv. Nuovo Cimento 1, 227 (1971).
[2]A. R. Bishop, K. Fesser, P. S. Lomdahl, W. C. Kerr, M. B. Williams, and S. E. Trullinger, Phys. Rev. Lett. **50**, 1095 (1983).
[3]A. R. Bishop, K. Fesser, P. S. Lomdahl, and S. E. Trullinger, Physica (Utrecht) **7D**, 259 (1983).
[4]A. R. Bishop and P. S. Lomdahl, Physica (Utrecht) **18D**, 54 (1986).
[5]D. W. McLaughlin and A. C. Scott, Phys. Rev. A **18**, 1652 (1978).
[6]A. C. Scott, Phys. Scr. **20**, 509 (1979).
[7]V. I. Karpman, Phys. Lett. **88A**, 207 (1982).
[8]O. H. Olsen and M. R. Samuelsen, Phys. Rev. A **23**, 3296 (1981).
[9]P. S. Lomdahl, O. H. Olsen, and M. R. Samuelsen, Phys. Rev. A **29**, 350 (1984).
[10]V. I. Karpman, N. A. Ryaboua, and V. V. Solov'ev, Phys. Lett. **92**, 255 (1982).
[11]M. Inoue and S. G. Chung, J. Phys. Soc. Jpn. **46**, 1594 (1979).
[12]M. Inoue, J. Phys. Soc. Jpn. **47**, 1723 (1979).
[13]D. W. McLaughlin and E. A. Overman II, Phys. Rev. A **26**, 3497 (1982).
[14]E. A. Overman II, D. W. McLaughlin, and A. R. Bishop, Physica (Utrecht) **19D**, 1 (1985).
[15]O. H. Olsen and M. R. Samuelsen, Phys. Rev. B **28**, 210 (1983).
[16]O. H. Olsen and M. R. Samuelsen, Phys. Rev. B **33**, 595 (1986).
[17]*Handbook of Mathematical Functions*, edited by M. Abramowitz and I. A. Stegun (Dover, New York, 1965).